International Journal of GEOMATE, June, 2025 Vol.28, Issue 130, pp.43-50
ISSN: 2186-2982 (P), 2186-2990 (O), Japan, DOI: https://doi.org/10.21660/2025.130.4823
Geotechnique, Construction Materials and Environment

ADVANCING CAPPING TECHNIQUES FOR EFFECTIVE RAINFALL INFILTRATION CONTROL USING CAPILLARY BARRIER SYSTEMS/FUNCTIONS

Hiiro Morikawa[1], *Shin-ich Kanazawa[2], Sota Yushima[1], Kira Iida[1]

[1] Environmental Science and Technology, Niigata University, Japan,
[2] Civil Engineering Program, Niigata University, Japan

*Corresponding Author, Received: 27 Nov. 2024, Revised: 12 Feb. 2025, Accepted: 13 Feb. 2025

ABSTRACT: Capillary barriers are a method of controlling rainfall infiltration. Specifically, it is created by layering a sand layer on top of a gravel layer due to the difference in water retention properties of the soil. Using this technique, infiltrating water in the soil, such as rainfall and groundwater, accumulates at the boundary of the two layers and flows naturally along the gradient. Capillary barriers are created from naturally occurring materials and have the advantages of excellent lateral drainage and economic efficiency. Specific applications include top covers for the final refuse disposal and the removed soil. Many laboratory experiments have been conducted on the limiting length of capillary barriers. However, there are few examples of numerical simulations on capillary barrier function, and the performance of the capillary barrier function has not been clarified. Therefore, in this study, rainfall infiltration analyses were conducted on model-scale and full-scale to explain the capillary barrier function's mechanism and evaluate and study its usefulness in full-scale ground. As a result, it was clarified that the total hydraulic head and suction realize the impervious function of the capillary barrier. It was also confirmed that the capillary barrier functions in both the model and full-scale ground and that the accumulation flow depends on the saturation of the ground.

Keywords: Capillary barrier functions, Geotechnical engineering, Numerical Analysis, Rainfall infiltration

1. INTRODUCTION

Capillary barriers (hereafter referred to as “CBs”) control the infiltration of rainfall into the ground. It is achieved by using two layers of soil materials with different grain sizes. Specifically, gravel is used as the lower layer and sand as the upper layer. Thus, CB is created by the difference in water holding capacity of the soil due to the two-layer structure. Using this method, infiltration of water in the soil, such as rainfall and groundwater, accumulates at the boundary of the two layers and flows down naturally along the slope of the boundary. This prevents seepage water from infiltrating into the ground below the CB, which is very inexpensive and has low environmental impact because it is produced by soil, and has the advantages of excellent lateral drainage, Durability from examples formed on the surface of ancient tombs, and permeability. Because of these advantages, CBs are being considered for use as top covers for final waste disposal sites, radioactive material storage facilities, and embankment structures as a countermeasure against groundwater and rainfall.

However, CBs are rarely constructed. This is because the mechanism of CB function, including breakthrough, has not been fully elucidated. Breakthrough is when the upper layer (fine-grained soil layer) can no longer hold a certain amount of water and begins to percolate downward into the lower layer (coarse-grained soil layer). The critical length is the horizontal length from the point where the infiltrated water in the fine-grained soil layer begins to flow down along the boundary of the material to the point where a breakthrough occurs. A long limit length of the CB means that the infiltrating water does not penetrate the coarse soil layer but flows down, so it is a very important factor in terms of the drainage performance of the CB and the infiltration suppression performance of the infiltrating water. Many studies on CB have focused on the critical length [1-6], material properties [1-3,6], and thickness of the CB layer [5] through laboratory experiments [1-6]. However, these experiments have the following problems: it is not possible to observe the conditions inside the ground, and in full-scale cases, the experiments cannot be easily conducted due to the large-scale standards.

Based on this research background, in this study, we conduct a numerical analysis simulation, which allows us to easily verify the CB on a model scale or a full-scale scale and understand the internal condition of the ground. We use numerical analysis to visualize the moisture state inside the ground using CBs of model ground composed of common materials and CBs of full-scale ground. Our research objectives were (1) to verify the usefulness of CBs at full scale, (2) to elucidate the interception mechanism of CB functions, and (3) to evaluate the performance of CB functions.

In the model ground, rainfall infiltration analysis considering slope gradient and rainfall intensity is

performed on the model ground and evaluated concerning (1) and (2).

In the full-scale case, rainfall infiltration analysis is conducted considering the case where CB is constructed as a top cover. In the case of full-scale ground, evaluate concerning (2) and (3).

2. RESEARCH SIGNIFICANCE

We believe that this research will clarify the usefulness of CB on a full scale, the performance of CB functions**,** and the mechanism of the CB function. In addition, numerical analysis will shed light on the changes in seepage water inside the ground that could not be determined through experiments. We believe that these will contribute to the determination of standards for high-performance CB structures and optimal materials. We also believe that CBs can be used as a method to stabilize the ground against rainfall infiltration since the CB technology allows rainfall to drain away without infiltrating into the ground.

3. RESEARCH METHODOLOGY

In this study, numerical analysis simulations are performed using an air-dissolved unsaturated soil/water/air-coupled finite analysis code (DACSAR-MP).

3.1 Air-Dissolved Unsaturated Soil / Water / Air Coupled Finite Analysis

3.1.1 About analysis code

Several unsaturated soil constitutive models have been proposed so far. This study uses the elasto-plastic constitutive model of unsaturated soil proposed by Ohno S., Kawai K., and Tachibana S. [7]. Ohno S., Kawai K. and Tachibana S. [8] proposed a model in which the effective saturation is the state quantity representing the stiffness, referring to the model in which the definition of the effective stress considering the water content of Karube D., Kato S., and Honda K. [9] is given.

Furthermore, it is widely known that the moisture characteristic curve (suction-saturation relationship), which determines the mechanical behavior of unsaturated soil, differs between dehydration and water absorption. In brief, there is not only one moisture characteristic curve that expresses the suction-saturation relationship but countless scanning curves depend on the water retention state during dehydration or water absorption. Based on that, Kawai K., Wang W., and Iizuka A. [10] proposed a moisture characteristic curve model that can express hysteresis by using the fact that these scanning curves have similar shapes during dehydration and water absorption. In addition to the model capable of hysteresis expression, this analysis code uses the logistic curve equation as shown in the figure. Here, Figure 1 is the "(1) dehydration curve" and "(2) water absorption curve" drawn on the dehydration side and the water absorption side from an arbitrary suction-saturation state, which is proposed by Sugii T. and Uno T. [11].

3.1.2 Finite element formulation

The governing equation in the unsaturated soil/water/air-coupled problem consists of the balanced ceremony, effective stress formula, unsaturated elasto-plastic constitutive equation, conformity expression, Darcy's rule, air Darcy's rule, continuous conditional expression, and continuous conditional expression considering gas phase. These formulas are given below.

・Balanced ceremony

$$\mathrm{div}\,\sigma^T + \rho g = 0, \sigma = \sigma^T \tag{1}$$

・Effective stress formula

$$\sigma' = \sigma^N + p_s 1,\ \sigma^N = \sigma - p_a 1 \tag{2}$$

・Unsaturated elasto-plastic constitutive equation

$$\dot{\sigma}' = D{:}\,\dot{\varepsilon} - C^s \dot{S}_e \tag{3}$$

・Conformity expression

$$\varepsilon = -\frac{1}{2}(\nabla u)^S \tag{4}$$

・Darcy's rule

$$\tilde{v} = -k \cdot \mathrm{grad}\, h \tag{5}$$

・Air Darcy's rule

$$\tilde{v}_a = -k_a \cdot \mathrm{grad}\, p_a \tag{6}$$

・Continuous conditional expression

$$n\dot{S}_r - S_r \dot{\varepsilon}_v + \mathrm{div}\,\tilde{\mathrm{v}} = 0 \tag{7}$$

・Continuous conditional expression considering gas phase

$$(1 - S_r)\dot{\varepsilon}_v + n\dot{S}_r - n(1 - S_r)\frac{\dot{p}_a}{K_a} - \mathrm{div}\tilde{\mathrm{v}}_a = 0 \tag{8}$$

Here, assuming that the saturation is a function that can be expressed only by suction, the following equation is obtained.

$$\dot{S}_r = \frac{dS_r}{ds}\dot{s} = -\frac{dS_r}{ds}\dot{p}_w \tag{9}$$

Furthermore, the increment of suction stress in Equation (2) is calculated by the following equation.

$$\dot{p}_s = \frac{1}{1 - S_{rc}}\left(\frac{dS_r}{ds}s + S_r - S_{rc}\right)\dot{s} \tag{10}$$

However, S_{rc} is the saturation degree indicated by the adsorbed aqueous phase and is a material constant.

Here, σ' is the effective stress tensor; σ^N is the base stress tensor; $\sigma$is the total stress tensor; p_s is the suction stress; p_a is the pore air pressure; D is the elastic stiffness tensor; ε is the strain tensor; C^s is the coefficient tensor; S_e is the effective degree of saturation; u is the displacement vector; $\tilde{v}$ is the flow velocity vector of interstitial water; k is the permeability coefficient tensor; h is all head; $S_r$is the degree of saturation; ε_v is the volumetric strain; n is the porosity; K_a is the air pressure; $\tilde{v}_a$ is the flow velocity vector of interstitial air; and the superscript s indicates the symmetric part of the tensor in ( ).

By weakly formalizing the above governing equation, discretizing it spatially and temporally, and solving it under the conditions of initial value and boundary value, the solutions of unknowns $\{\Delta u^N\}$, $\{\Delta h^N|_{t=t+\Delta t}\}$, and $\{\Delta p_a^N|_{t=t+\Delta t}\}$ can be obtained.

Here, Δu^N is the amount of change in node displacement; Δh^N is the amount of change in total water head in minute time Δt; Δp_a^N is the amount of change in air pressure in a minute time Δt.

3.2 Infiltration analysis of model-scale

3.2.1 Analysis model

Figure 2 shows the analytical model（model ground）. The model ground is 110 cm wide and 50 cm high. Different soil materials are placed in the bottom 10 cm and top 40 cm of the model ground. The bottom is a coarse-grained soil layer, and the top is a fine-grained soil layer. In this analysis, the model ground is given a slope after it is created. The model ground specifications are based on based on the experiments.[1-6]

3.2.2 Analysis conditions

The soil materials used are the commonly used fine-grained and coarse-grained soils, sand and gravel, respectively, and the initial degree of saturation is set to 60%. Tables 1 and 2 show the material constants of the sand and gravel, and Figures 3 and 4 show the moisture-characteristic curves of the sand and gravel. Regarding the material parameters, λ is the expansion index; κ is the compression index; M is the limit state parameter; m is the unsaturated permeability coefficient of Mualem [12], n is the E_c model parameter; n_E is the enlargement ratio of yield surface; ν is the Poisson's ratio; e_0 is the initial void ratio; S_{r0} is the initial degree of saturation; $k_{x,y}$ is the hydraulic conductivity [m/sec], $k_{ax,ay}$ is the coefficient of air permeability [m/sec], ρ_s is the soil particle density [t/m^3], ρ_t is the wet density[t/m^3] and ρ_a is the air density [t/m^3]. The boundary conditions are full ventilation, with only the coarse-grained soil part on the left side being a drained boundary, and the rest being undrained boundaries.

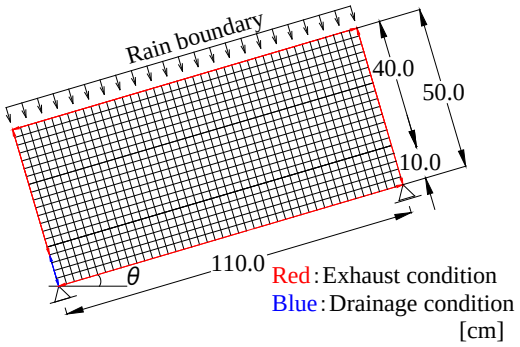

Fig. 2 Analysis model (Model-scale)

Table. 1 Material parameters (Sand)

λ	κ		M	m
0.10	0.010		1.375	0.67
n	n_E	e_0	ν	S_{r0}
1.0	1.3	1.0	0.33	0.073
$k_{x,y}$ $[m/day]$	$k_{ax,ay}$ $[m/day]$	$\rho_t[t/m^3]$	$\rho_a[t/m^3]$	$\rho_s[t/m^3]$
1.12×10^1	1.12×10^3	1.8	1.2×10^{-3}	3.0

Table. 2 Material parameters (Gravel)

λ	κ		M	m
0.05	0.005		1.375	0.57
n	n_E	e_0	ν	S_{r0}
1.0	1.3	0.84	0.33	0.013
$k_{x,y}$ $[m/day]$	$k_{ax,ay}$ $[m/day]$	$\rho_t[t/m^3]$	$\rho_a[t/m^3]$	$\rho_s[t/m^3]$
2.85×10^2	2.85×10^4	1.692	1.2×10^{-3}	2.610

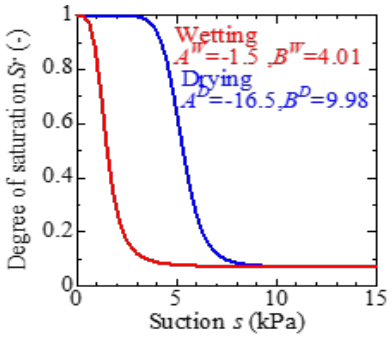

Fig. 3 Moisture characteristic curve (Sand)

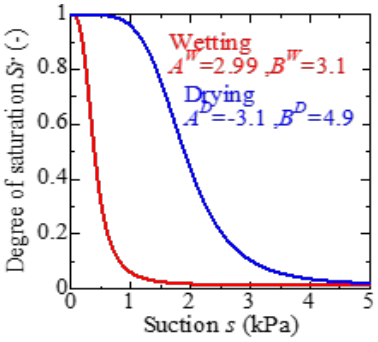

Fig. 4 Moisture characteristic curve **(**Gravel)

3.2.3 Analytical method

The model ground is subjected to a slope gradient (10°, 20°, 30°) and rainfall (15mm/h, 25mm/h) for 24 hours, and then left for 24 hours. The rainfall is applied only to the top surface of the model ground with a constant rainfall intensity. Regarding the gradient, we will verify the gradient from gentle to steep, which has not been examined much in past studies [1-6]. In addition, we will assume normal rainfall.

3.3 Infiltration analysis of full-scale

3.3.1 Analysis model

Figure 5 shows the analysis model (full-scale ground). The full-scale ground is assumed to be the top cover of a final disposal site. The full-scale ground is 20m wide and 1.4m high. The bottom 0.2m is a coarse-grained soil layer, and the upper 0.2m is a fine-grained soil layer. The gradient of the boundary between the coarse-grained soil layer and the fine-grained soil layer is 10% (approximately 5.7°). The full-scale specifications are based on the experiments [1-6].

3.3.2 Analysis conditions

The soil materials used are sand and gravel, the same as those used in the model ground. The initial degree of saturation of the full-scale ground is 60%. After construction, a period of leaving the ground is allowed to reach a steady state.

3.3.3 Analytical method

After the elements of full-scale ground are generated, a period is set aside to allow the saturation level in the ground to reach a steady state. After that, rainfall (7mm/h) is applied for 24 hours, and the ground is left to stand for another 24 hours. Rainfall is applied at a constant intensity only on the top surface of the model ground. In this analysis, multiple rainfalls were applied in advance for verification. The reason for applying a rainfall intensity of 7mm/h was that this was the limit rainfall intensity at which CB could almost completely block water.

4. RESULTS AND CONSIDERATIONS

4.1 Infiltration analysis of model-scale

Figure 6 shows the change in degree of saturation over time for each slope gradient at a rainfall intensity of 15 mm/h. Figure 7 shows the contour map of saturation degree for each rainfall intensity, Figure 8 shows the contour map of the total water head for each rainfall intensity, and Figure 9 shows the contour map of suction for each rainfall intensity. Figure 6 shows the saturation degrees 3, 12, 24, 27, 36, and 48 hours after the start of rainfall.

The results of this analysis are similar to those of the study by Sawada et al. [4] ([4] conducted experiments with gradients of 5° and 10° and rainfall intensities of 4mm/h and 8mm/h, respectively).

4.1.1 Usefulness of CB Functions

Figures 5 and 6 show that for each slope gradient, rainwater seeping through the fine soil layer becomes a sediment flow at the boundary between the coarse soil layer and the fine soil layer and flows down the slope. After rainfall, water flows down the slope and a breakthrough is observed near the drainage boundary, confirming that it is being drained. Therefore, it can be said that the CB is functioning for each slope gradient.

In addition, the saturation distribution 24 hours after the start of rainfall is almost the same for each slope gradient from the start to the end of rainfall, which is thought to be due to the high permeability, and the high hydraulic conductivity of the soil material used in this analysis. As a result, rainfall quickly falls and seeps down, so it is thought that the amount of water flowing in and the amount of water draining out are very similar.

4.1.2 Mechanism CB Functions

Figure 7 shows that the degree of saturation immediately after the end of rainfall to immediately after the end of analysis was higher in the fine soil layer than in the coarse soil layer, for both rainfall intensities of 15mm/h and 25mm/h. This is thought to be due to the effects of total head and suction. In Figure 8, the total head for each gradient is significantly different at the boundary between the coarse soil layer and the fine soil layer. It is thought that this head difference causes the flow lines perpendicular to the equipotential lines to bend in the direction of the boundary gradient. Regarding suction, it is said that when the suction of the lower layer is lower than that of the upper layer in an unsaturated

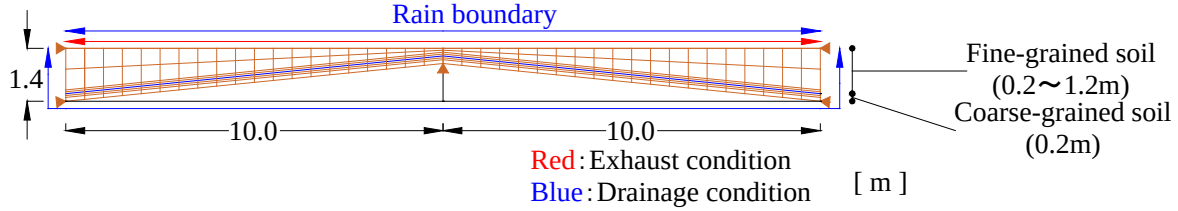

Fig. 5 Analysis model (Full-scale)

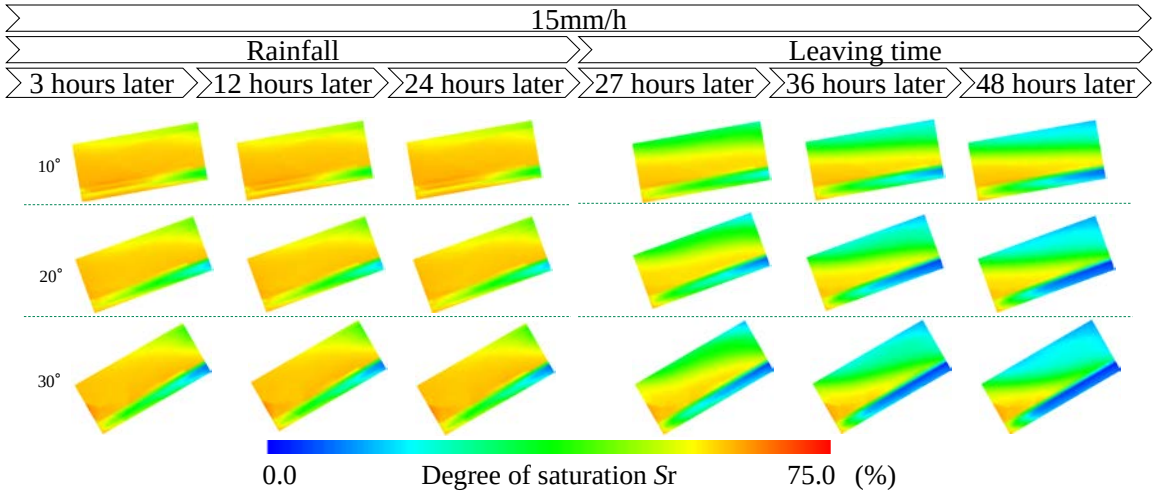

Fig. 6 Change in saturation over time for a rainfall intensity of 15 mm/h

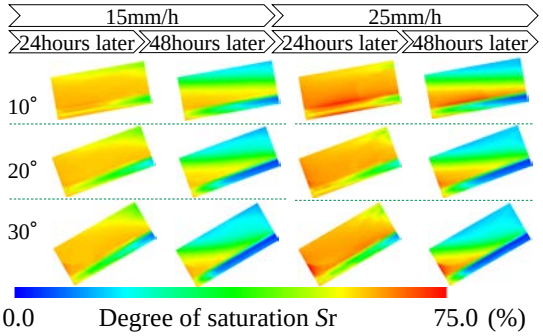

Fig. 7 Degree of saturation S_r

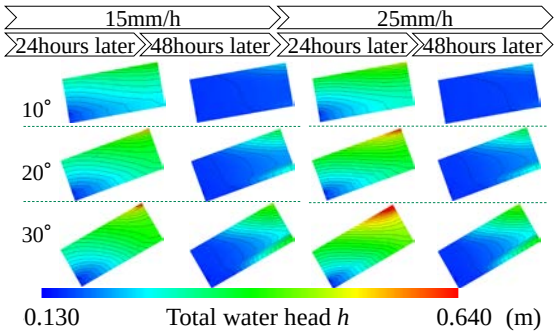

Fig. 8 Total water head *h*

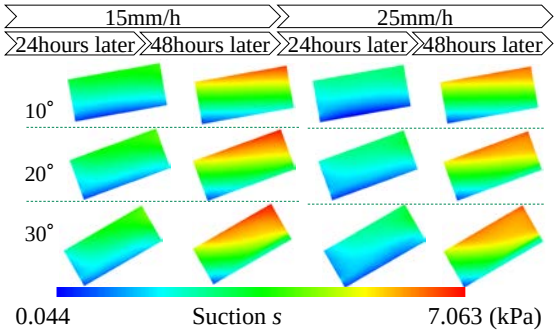

Fig. 9 Suction *s*

state, the infiltrated water will remain in the upper layer and will not infiltrate into the lower layer. Figure 7-9 shows that the ground analyzed was unsaturated, and the equipotential lines are bent at the boundary between the coarse soil layer and the fine soil layer, so it is thought that the CB function is suppressing the infiltration of accumulated flow into the coarse soil layer.

4.1.3 Performance of CB Functions

From Fig. 7, it can be seen that immediately after the end of rainfall, the highly saturated area of the fine soil layer with a gradient of **30**° is located closer to the drainage boundary than the highly saturated area of the fine soil layer with a gradient of **10**°, regardless of the rainfall intensity. The highly saturated area of the coarse soil layer is distributed closer to the drainage boundary with a gradient of **30**° than with a gradient of **10**°. In addition, the highly saturated zone of the fine soil immediately after the end of the analysis is smaller with a gradient of **30**° than with a gradient of **10**°. These suggest that the steeper the gradient, the more the breakthrough position extends, and the more rainfall infiltration into the coarse soil is suppressed, resulting in better drainage. Furthermore, high permeability also affects drainage performance. In particular, in Fig. 4, the steeper the gradient, the greater the change in the total head at the boundary between the coarse soil layer and the fine soil layer, both after rainfall and after leaving it. Also, the greater the gradient, the narrower the interval between the equipotential lines. As a result, since the flow lines move toward the drainage boundary, it is believed that the greater the gradient, the better the drainage performance and infiltration prevention performance.

4.2 Infiltration Analysis of Full-Scale

In the following, since the full-scale ground is a bilaterally symmetrical model, only the results for the left half are shown.

Figure 10 shows the element numbers and their locations that are the focus of this analysis. Figure 11 shows a contour map of the degree of saturation of the

full-scale ground that is left for 10 days (240 hours) after the elements are generated. Figures 12 show the change in the degree of saturation over time for a certain element number. Figure 13 shows the change in the degree of saturation over time for a full-scale ground that is given rainfall (7mm/h) from a steady state. Figure 13 shows the change over time of the saturation of the full-scale ground that was subjected to rainfall (7 mm/h) for 24 hours from a steady state and then left for 24 hours. Figure 14 shows the change over time in saturation for a given element number (including the period before steady state). Figure 15 shows the change over time of the total hydraulic head of the full-scale ground that was subjected to rainfall (7 mm/h) for 24 hours from a steady state and then left for 24 hours.

4.2.1 Bringing the actual ground to a steady state

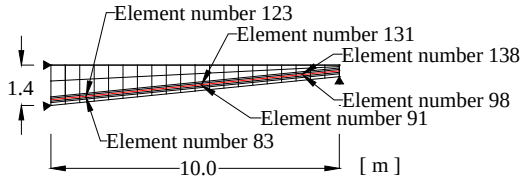

Fig. 10 Each element number and its location

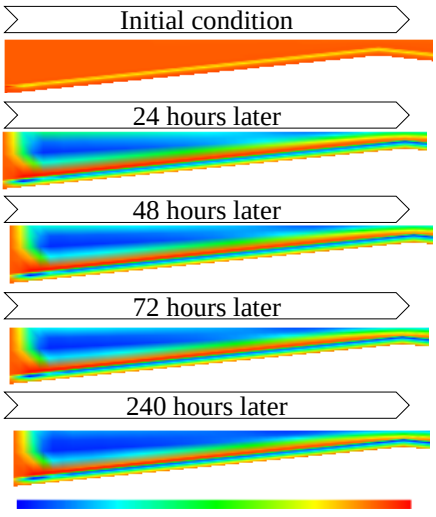

Fig. 11 Degree of saturation S_r (%)

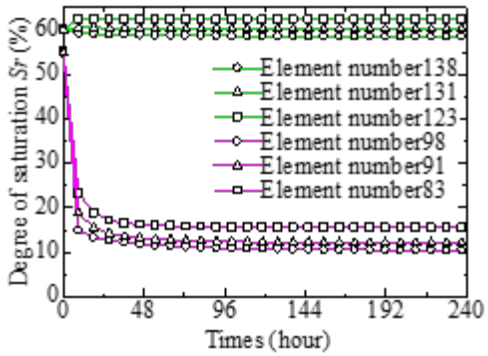

Fig. 12 Degree of saturation S_r (%)

As shown in Figure 11, the degree of saturation decreased from the initial state, and the saturation distribution of the entire analysis model became uniform about 10 days after the start of the analysis. The change in the degree of saturation of each element over time is gradual, and almost no change in the degree of saturation is observed 10 days after the start of the analysis. For this reason, the degree of saturation 10 days after the generation of the full-scale ground elements is adopted as the steady state.

4.2.2 Usefulness of CB function in full-scale ground

It can be seen from Figure 14 that the degree of saturation at the boundaries of the soil layers increases significantly when rain is applied from a steady state. During the period when the rainfall stops and the soil is left to stand, the increased degree of saturation decreases. Looking at the change in saturation for each element in Figures 16-18, the elements of the fine soil layer experience a large increase in saturation due to rainfall, whereas the elements of the coarse soil layer do not show a similar increase in saturation. This suggests that the CB is functioning on a full scale and that it is effective under the same conditions.

4.2.3 Full-scale CB during rainfall and leaving times

Figure 13 shows that the degree of saturation of the fine soil at the boundary of the soil layers increases significantly over time due to rainfall, but the degree of saturation of the fine soil layer above the boundary of the soil layers is low. This is thought to be because the increase in the saturation of the ground is not a direct result of rainfall, but rather a result of the large amount of rainfall flowing from the upstream side of the accumulation flow. In addition, because the increase in the degree of saturation of the fine soil at the boundary of the soil layers is confirmed from the upstream side of the accumulation flow, it was confirmed that the accumulation flow occurs from the top of the gradient.

Figure 13 shows that focusing on the period of neglect after rainfall, the degree of saturation of the fine soil, except for the fine soil at the boundary between soil layers, has decreased. In particular, the degree of saturation of the fine soil on the upstream side of the accumulated flow has decreased significantly. Figure 14 shows that the degree of saturation of the fine soil at the boundary between soil layers has also decreased, indicating that the accumulated flow disappears from the upstream side.

4.2.4 Equipotential lines and accumulated flow

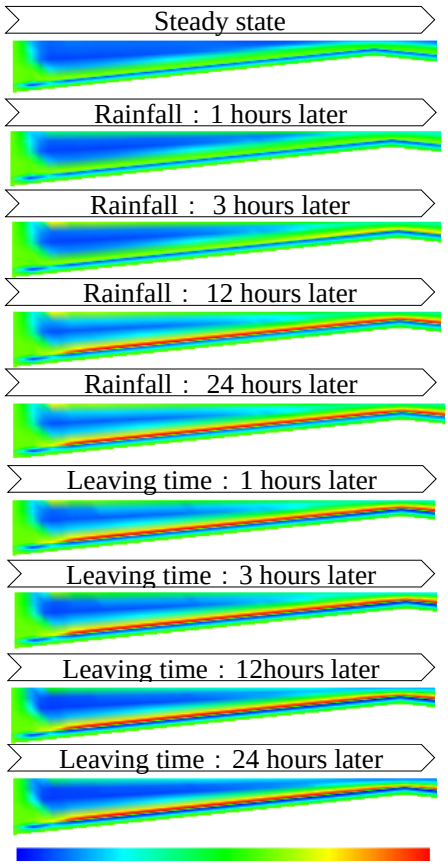

Fig. 13 Degree of saturation S_r (%)

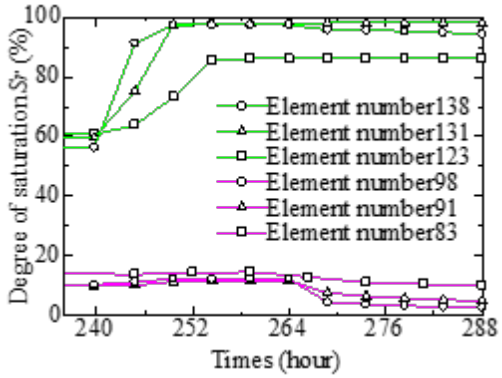

Fig. 14 Degree of saturation S_r

Figure 15 shows that from the steady state, the total water head of the fine soil layer is greater than that of the coarse soil layer, but the difference in total water head between the coarse soil layer and the fine soil layer increases due to rainfall. As this head difference increases, the interval between the equipotential lines narrows and the bending of the equipotential lines increases. Comparing Figures 14 and 20, the accumulation flow can be confirmed in the saturation distribution three hours after the start of rainfall, but at the total water head of the point where the accumulation flow is occurring, the equipotential lines overlap with adjacent equipotential lines due to bending. After that, just as the accumulation flow

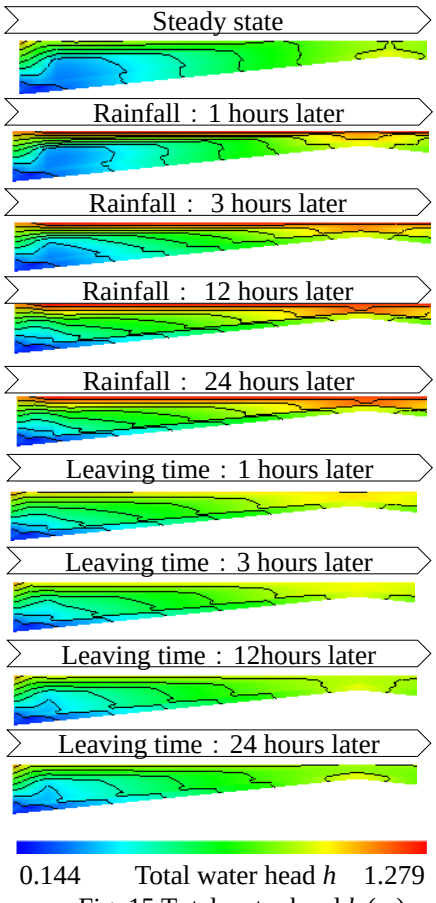

Fig. 15 Total water head h (m)

becomes longer, the number of points where the equipotential lines overlap increases.

Figure 15 shows that after the rainfall ends, the seepage water in the ground is drained, and at the same time, the difference in total water head between the coarse soil layer and the fine soil layer decreases and the interval between the equipotential lines increases. This shows that when the accumulation flow disappears, the equipotential lines no longer overlap.

5. CONCLUSION

The findings obtained are described below according to the research objectives.

(1) I is found that CB is effective in both the model-scale and the full-scale.

(2) It is found that the total water head and suction exert the CB function. First, regarding the total water head, it is thought that by using different soil materials, a sudden change in the total water head occurred at the boundary between the materials, causing the flow line in the model ground to bend. In addition, regarding suction, since the model ground is composed of highly permeable materials, it is prone to becoming unsaturated, and since the suction is relatively larger at the top of the model ground than at the bottom, it is thought that the infiltrating water is

easily retained at the top. Since these are affected by the moisture properties of the soil, it is suggested that CB will be exhibited if the structure is composed of materials with significantly different moisture properties.

(3) The higher the rainfall intensity, the larger the distribution of high saturation in fine-grained soil becomes, but the distribution of saturation is relatively uniform during rainfall. This indicates that if the rainfall duration is constant, the trend does not change even if the rainfall intensity changes. After rainfall, the high saturation zone in fine-grained soil shrinks. It was found that the influencing factor of this performance is the gradient. It is found that the greater the gradient, the easier it is for the infiltrated water to flow down as an accumulated flow, and that it becomes easier to reuse as a CB after the rainfall has stopped. It is also found that the accumulated flow can be confirmed from the total water head. In this case, the equipotential line is bent so that it overlaps with the adjacent equipotential line. It is found that the accumulated flow starts at the apex of the soil layer boundary, and when the accumulated flow disappears, it disappears from the upstream side of the soil layer boundary.

Considering these points, when considering the actual use of CB, the non-uniformity of the material may change the moisture characteristics of the fine-grained soil layer and the entire coarse-grained soil layer. Therefore, it is necessary to use a uniform material. Also, when using CB on flat ground, it is considered that the gradient at the boundary between the materials should not be too large. This is because the CB will expand in the vertical direction as the gradient becomes larger. Thus, the CB should be constructed of a uniform material, and if on flat ground, it should be constructed with a steep gradient that satisfies the buried capacity of the bottom of the top cover.

Our future plans include conducting full-scale CB experiments, which will allow us to compare the results of this analysis with those of the experiments.

6. ACKNOWLEDGMENTS

Many people cooperated with this research, and I would like to express my sincere gratitude to Professor Kanazawa.

7. REFERENCES

[1] Kaoru K, Kazunobu M, Asuka S, Toshihiro M., A study on fine-grained soil suitable for maximizing the limit length of capillary barrier-type soil cover, Proceedings of the Japan Society of Civil Engineers C, Vol. 76, 2020 pp. 215-220,

[2] Nakafusa S, Kobayashi K, Morii T, Nishimura T., Alternative Employment of Crushed Shell Particles in Capillary Barrier of Soil, Int. J. of GEOMATE, Vol. 1, No.1 (Sl. No. 1), 2011, pp. 50-55, Geotec., Const. Mat. and Env., ISSN:2186-2982(P), 2186-2990(O), Japan.

[3] Taketo S, Takaki M, Application of capillary barrier type soil cover, Journal of the Japan Society of Civil Engineers, Vol. 78, No. 3, 2022. pp. 180-196,

[4] Mai S, Mamoru M, Mitsugu Y, A Study on Rainwater Infiltration Control in Ancient Mounds Using Capillary Barriers - Experimental and Analytical Investigation of Capillary Barrier Mechanisms - Journal of the Japan Society of Civil Engineers, C (Geotechnical Engineering) 72 (2), 2016, pp. 101-116,

[5] Nakafusa S, Kobayashi K, Morii T, Nishimura T, Alternative Employment of Crushed Shell Particles in Capillary Barrier of Soil, Int. J. of GEOMATE, Oct. 2011, Vol. 1, No.1 (Sl. No. 1), pp. 50-55, Geotec., Const. Mat. and Env., ISSN:2186-2982(P), 2186-2990(O), Japan

[6] Study of water flow and retention in clay-sand liners , International Journal of GEOMATE, March., 2018 Vol.14, Issue 43, pp.83-90, Geotec., Const. Mat. & Env. ISSN: 2186-2982 (Print), 2186-2990 (Online), Japan

[7] Kanazawa, M., Toyoshima, K., Kawai, I., Tachibana, M., and Iizuka, A.: Analysis of mechanical behavior of compacted soil by FE method, Journal of Japan Society of Civil Engineers, Vol. 68 (2), 2012, pp. 291-298.

[8] Makoto O, Isao K, Makoto T, An elastoplastic constitutive model for unsaturated soils using effective degree of saturation as a stiffness parameter, Journal of the Japan Society of Civil Engineers, Vol. 63/No. 4, 2007, pp. 1132-1141.

[9] Daisuke K, Makoto K, Kazuyuki H and Masaharu H, Relationship between mechanical behavior of unsaturated soil and state of pore water, Journal of Japan Society of Civil Engineers, Vol. 535 /III-34, 1996, pp. 83-92.

[10] Isao K, Wei W, Akira I. Expression of hysteresis appearing in water characteristic curve and stress change of unsaturated soil, Journal of Applied Mechanics, Vol. 5, 2002, pp. 777-784.

[11] Sugii T, Takafumi U, New modeling of moisture characteristic curve, Journal of Japan Society of Civil Engineers, 1995, pp.130-131.

[12] Muallem, Y. A new model for predicting hydraulic conductivity Unsaturated Porous Media, Water Resources Research, Vol. 12, No. 3, 1976, pp. 514-522.